Towards sustainability: a new, solid-state synthetic route for supported metal nanocatalysts

Udishnu Sanyal, Suresh Babu Kalidindi, Sharika Nair and Balaji R. Jagirdar*

Department of Inorganic and Physical Chemistry, Indian Institute of Science, Bangalore 560 012, India

Noble metal ions like Pt(IV) and Pd(II) were impregnated on γ-alumina and aerosol 300 silica surfaces. Reduction of these ions using ammonia borane in the solid state resulted in the formation of the respective metal nanoparticles embedded in BNH_x polymer which is dispersed on the oxide support. Removal of the BNH_x polymer was accomplished by washing the samples repeatedly with methanol. In this process the polymer undergoes solvolysis to release H_2 accompanied by the formation of ammonium methoxy borate salt, which has been removed by repeated methanol washings. As a result, metal nanoparticles well dispersed on γ-alumina and aerosol 300 silica were obtained. These samples have been characterized by a combination of techniques, including electron microscopy, powder X-ray diffraction, NMR spectroscopy and surface area analyser.

Keywords: Alumina, nanocatalysts, noble metal ions, silica.

Introduction

OVER the last 30 years, nanomaterials, especially metal nanoparticles, have been intensively studied not only due to their fundamental scientific interest, but also due to the many technological applications that they have to offer[1–3]. Some of the challenges in the area of metal nanoparticles, in particular, to exploit their special catalytic properties in the nano-size regimes include their stabilization and immobilization to facilitate their easy recovery and reuse. The issue of stability was largely addressed and sorted out by employing organic and inorganic capping ligands, surfactants and polymers[4,5]. However, the catalytic activity gets affected, and the recovery of the catalyst and then reuse are fraught with difficulties. Most often it has been found that the catalytically active sites are blocked by the organic ligands and also the nanoparticles undergo agglomeration with time under the reaction conditions employed and therefore, lose their catalytic activity[6]. These issues could be circumvented to a great extent by employing support materials as host materials for metal nanoparticles.

Supported metal nanoparticles as catalytic systems have potential to show greater efficiency. And in combination with the advantages of the heterogeneous support, they could also exhibit high selectivity, lead to an increased overall conversion and afford higher yield. The catalyst recovery in this case is easy; a simple filtration results in a complete recovery of the catalyst. The unique properties of the supported metal nanoparticles or clusters are a result of their particle size/shape, metal dispersion, and the electronic properties of the metal nanoparticles in relation to their support[7]. Transformation of bulk gold, considered as the most inert member of the noble metal family, to a highly active catalytic centre for CO oxidation when the size is reduced to the nanoregime on an appropriate support, remains one of the most remarkable examples towards this direction[8].

Among the various metal nanoparticles, the noble metal nanomaterials on oxide supports are of great interest in the field of heterogeneous catalysis due to their unique physical and chemical properties[9,10]. A unique combination of metal and support is often required to enhance the activity, selectivity and stability. The conventional preparation methods for metal nanoparticles on supports such as co-precipitation, impregnation and chemical vapour deposition afford metal nanoparticles with a broad size distribution[11,12]; uniform-sized metal nanoparticles are obtained only at extremely low loadings[13–15]. Alternatively, colloidal metal nanoparticles could be grafted on suitable supports, wherein the surfactant or the polymer prevents agglomeration of the particles[16–18]. The catalytic activity, however, is hampered by the presence of surfactant molecules or polymer agents which block the active sites on the catalyst. Thus it remains a challenging task to realize monodispersed nanoparticles on supports, especially at high loadings.

We recently reported that ammonia borane ($H_3N \cdot BH_3$, AB) reduces various metal salts in aqueous medium or in methanol along with the release of H_2, resulting in the formation of metal or metal boride nanoparticles[19,20]. We also found that the synthesis of metal nanoparticles can be accomplished in the solid state. In this case, AB acts a reducing agent and simultaneously releases H_2 accompa-

nied by the formation of BNH_x polymer, which halts the growth of the particles[21,22]. Ammonia borane plays a dual role: as a reducing agent as well as a precursor of the stabilizing agent and thereby brings about an atom economy in the overall process. With a view to obtain metal nanoparticles supported on suitable oxide supports for catalytic applications, we attempted the synthesis of alumina (Al_2O_3) and silica (SiO_2)-supported Pt and Pd nanoparticles using AB as the reducing agent in the solid state. Here, we report the results of these studies.

Experimental section

Materials

Aerosil 300 silica (Degussa; A300) and γ-alumina were purchased from Evonik and Sigma Aldrich respectively. Methanol, $Pd(OCOCH_3)_2$ and H_2PtCl_6 were purchased from S.D. Fine Chemicals, India. AB was synthesized from $(NH_4)_2SO_4$ and $NaBH_4$ in ~90% yields using the procedure described by Ramachandran and Gagare[23]. The purity of AB was established by ^{11}B NMR before use. The transmission electron microscopy (TEM) samples were prepared by sonicating the nanopowders in THF for 5 min before placing the samples on a Formvar-coated copper grid of 300 mesh. The TEM bright-field (BF) images and high-resolution TEM (HRTEM) images were obtained using TECHNAI T20 transmission electron microscope operating at 200 kV. Avance Bruker 400 MHz NMR spectrometer was used for recording the ^{11}B NMR spectra. Powder X-ray diffraction measurements were carried out using Bruker D8 ADVANCE diffractometer. Brunauer–Emmett–Teller (BET) surface-area measurements of the samples were carried out using a Micromeritics surface area analyser model ASAP 2020. The samples were degassed at 100°C for 4 h under vacuum and measurements were carried out by N_2 adsorption at 77 K.

Methods

Preparation of Al_2O_3-supported Pt nanoparticles

In a 100 ml round-bottom flask equipped with a magnetic stirrer bar, 0.8 g (7.84 mmol) of Al_2O_3 was taken. To this 20 ml of methanol was added and then sonicated for 5–10 min to make a slurry of Al_2O_3. Then, chloroplatinic acid (0.083 g, 0.20 mmol) was added to it and stirred vigorously for 2 h at room temperature. The colour of the slurry turned light yellow from white. The solvent was removed *in vacuo* to obtain a light yellow-coloured powder. Then, 0.031 g (1 mmol) of AB was added to this powder and the reaction mixture was stirred vigorously for 8 h under N_2 atmosphere without any solvent. The colour of the powder changed to black during the addition of AB.

After completion of the reaction, a black-coloured powder was collected and washed with methanol two times. Finally, the powder consisting of 5 wt% Pt on Al_2O_3 was washed with diethyl ether and dried under vacuum.

Preparation of Al_2O_3-supported Pd nanoparticles

The preparation of Pd/Al_2O_3 was carried out in a similar manner to that of Pt/Al_2O_3. To obtain 5 wt% Pd on Al_2O_3, 0.8 g (7.84 mmol) of Al_2O_3 and 0.084 g (0.4 mmol) of palladium acetate ($Pd(OCOCH_3)_2$) were taken. To a dark yellow-coloured mixture of $Pd(OCOCH_3)_2$ and Al_2O_3, 0.062 g (2 mmol) of AB was added and stirred vigorously for 8 h under nitrogen atmosphere without any solvent. The colour of the powder changed from dark yellow to black. After completion of the reaction, black-coloured powder was collected and washed with methanol two times. The Pd/Al_2O_3 powder was finally washed with diethyl ether and dried under vacuum.

### Preparation of SiO_2-supported Pt nanoparticles

In a 100 ml round-bottom flask equipped with a magnetic stirrer bar, 0.8 g (29 mmol) of silica was taken. To this 20 ml of methanol was added and sonicated for 5 min to make a slurry of silica. To this slurry, 0.083 g (0.2 mmol) of H_2PtCl_6 was added and stirred vigorously for 2 h at room temperature, after which time the solvent was removed *in vacuo*. To the resulting powder, 0.031 g (1 mmol) of AB was added and stirred vigorously for 8 h. During this time the colour of the powder changed from light yellow to black. The black powder of 5 wt% Pt on SiO_2 was isolated after washing with methanol.

Preparation of SiO_2-supported Pd nanoparticles

The preparation of Pd nanoparticles supported on SiO_2 was carried out in a similar manner to that of Pt on silica. In this case, a slurry of 0.8 g (29 mmol) of silica in 20 ml of methanol was made. $Pd(OCOCH_3)_2$ (0.084 g, 0.4 mmol) was added to this slurry and stirred for 2 h. The solvent was removed completely *in vacuo* to obtain a dark yellow-coloured powder. To this powder, 0.062 g (2 mmol) of AB was added which resulted in a black-coloured reaction mixture. This powder consisting of 5 wt% Pd on silica was collected and washed with methanol three times and finally dried under vacuum.

Results

Supported metal nanoclusters are an important class of materials in the field of heterogeneous catalysis because of their unique structure–activity relationship. Among these, the noble metal catalysts are of great interest and have significant applications on an industrial scale[10,24–26].
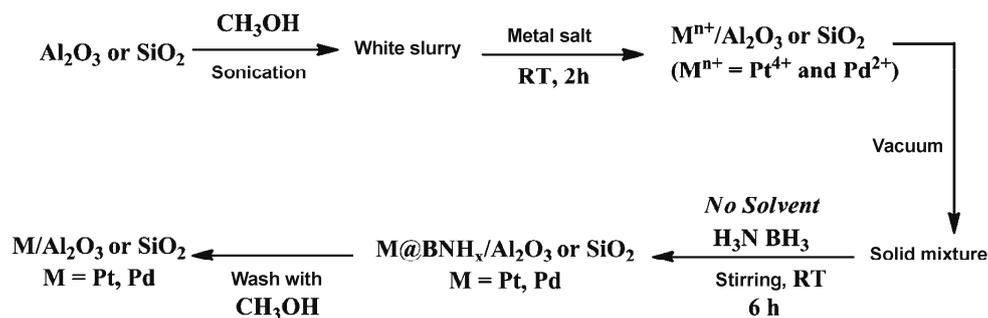
Scheme 1. Reaction sequence for the synthesis of supported metal nanoparticles.

In view of the high cost of noble metals, recovery of the catalyst assumes immense importance. Thus, metal catalysts supported on suitable supports are significant since recovery of the catalyst could be achieved via simple filtration processes.

In the supported metal catalysts, the metal is present in a finely dispersed form in small quantities on a high-surface-area metal oxide support. Supported metal catalysts are typically made by the impregnation of support with an aqueous solution of metal salt followed by calcination (heating in air) or reduction with hydrogen[27–29]. Then the metal particles are distributed on the internal surface of the support. Here, we report a new solid-state route for the synthesis of Pt and Pd nanoparticles supported on alumina as well as silica from the respective metal salts using AB as the reducing agent. In this case, first the metal ions (typically in their metal salt form) were adsorbed on the surface of the solid support by a conventional wet impregnation method and then the metal ions were reduced by AB in a solid-state method to obtain metal nanoparticles dispersed on the solid support. We used the support materials such as γ-Al_2O_3 and aerosil 300 SiO_2 as slurries in methanol for dispersing the metal salts, H_2PtCl_6 and $Pd(OAc)_2$. Removal of the solvent gave powders which contained Pt^{4+} and Pd^{2+} adsorbed on silica and alumina. The colours of the powders obtained were light yellow and dark yellow in case of Pt^{4+} and Pd^{2+} respectively.

These powders were treated with AB (AB/metal ratio = 5) in the solid state. The reactions were preceded by instantaneous colour change from light and dark yellow to black in the case of Pt and Pd respectively. Stirring was carried out for 6 h, which was found to be optimum for the completion of the reaction. After the reaction, the black powder obtained was composed of the metal nanoparticles stabilized by the BNH_x polymers and supported on Al_2O_3 or SiO_2. Washing of these materials with methanol several times rendered the complete removal of the BNH_x polymer. The resulting powder was found to be comprised of metal nanoparticles supported on Al_2O_3 or SiO_2, as evidenced by various characterization techniques (see below). The complete reaction sequence is shown in Scheme 1.

Alumina-supported Pd and Pt nanoparticles

The morphology of the catalyst was examined using TEM. The black nanopowder obtained in each case (Pd and Pt) was repeatedly washed with methanol and then redispersed in THF by sonication, and samples for TEM were made by placing 2 μl sample on a carbon-coated Cu grid. The TEM bright field image (Figure 1 *a*) as well as the high-angle annular dark-field scanning transmission electron microscopy (HAADF-STEM) images (Figure 1 *e*) of the Pd/Al_2O_3 catalyst revealed the presence of Pd nanoparticles on the alumina surface. No regions of unsupported Pd nanoparticles were found in the grid. The particles were nearly agglomerated; however, we could estimate the particle size from the HRTEM images (Figure 1 *b*). The HRTEM image shows that each aggregate is comprised of smaller sized (~4–5 nm) Pd nanoparticles. From the EDX analysis (Figure 1 *c*), we found that the quantity of Pd present in the sample is 6.4 wt%. Since the reflections of Pd are under those of γ-Al_2O_3, unambiguous assignment of the powder XRD peaks (Figure 1 *d*) to those of Pd was not straightforward. This was compounded by the very small quantity of Pd present in the sample.

On the other hand, the TEM BF image (Figure 2 *a*) and HAADF-STEM image (Figure 2 *e*) of Pt/Al_2O_3 sample revealed the presence of Pt nanoparticles on the alumina surface. Here too we did not find bare Pt nanoparticles in any region of the grid; only Pt-supported on Al_2O_3. The BF image showed only agglomerated particles on γ-alumina spheres of 100–200 nm diameter. The HRTEM image (Figure 2 *b*), however, evidenced the presence of smaller sized Pt particles (5–6 nm) within the agglomerated regions. The crystalline nature of both Pt nanoparticles and alumina was quite evident from the HRTEM image. In addition, the HRTEM image showed lattice fringes corresponding to the (111) plane of FCC Pt with a *d*-spacing of 2.24 Å. The EDX analysis (Figure 2 *c*) further confirmed the presence of Pt of 4.9 wt%. As in the case of Pd/Al_2O_3, we could not unambiguously assign the peaks due to Pt in the powder XRD pattern (Figure 2 *d*) of Pt/Al_2O_3 due to overlap of the reflections of γ-Al_2O_3 with those of Pt. Here as well, the Pt content is quite small.
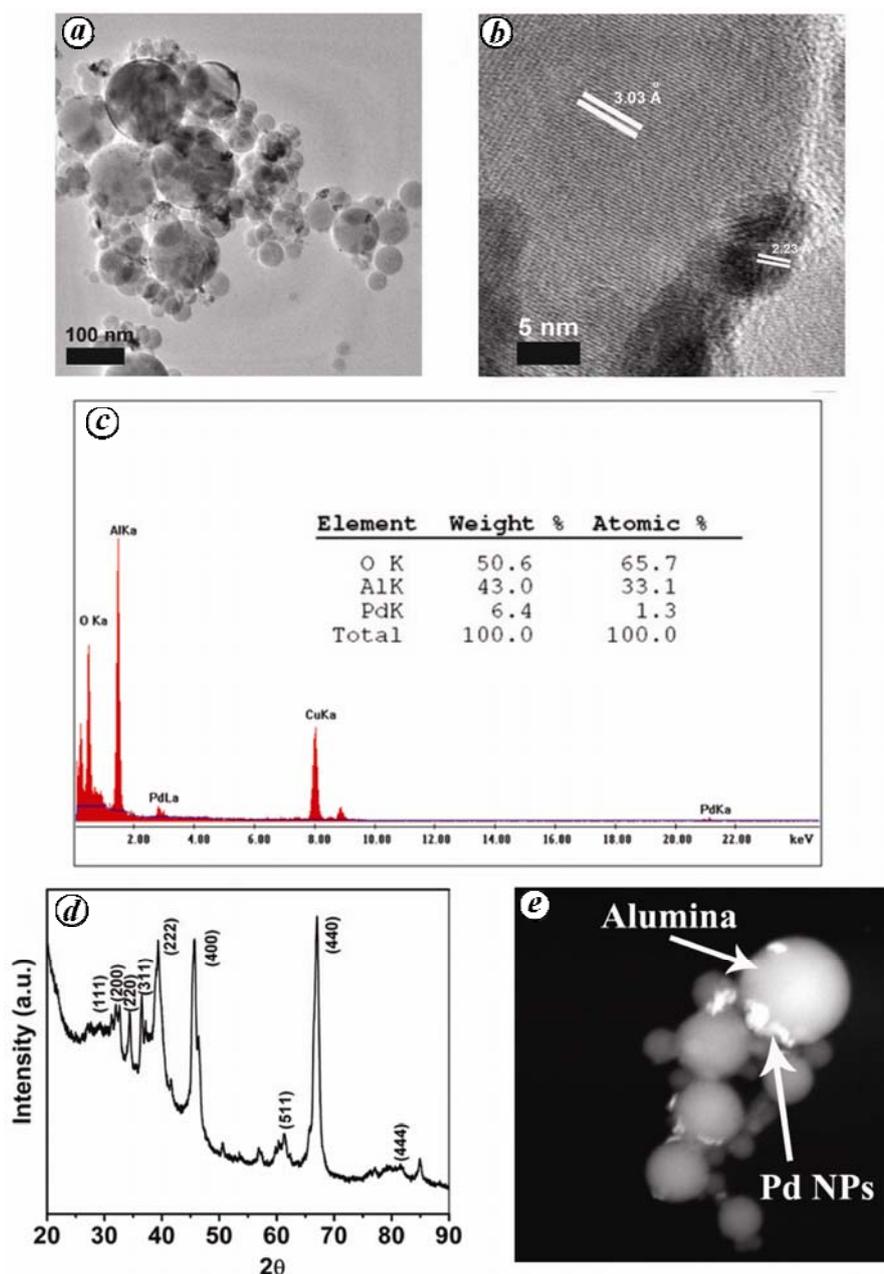
Figure 1. Pd/Al$_2$O$_3$ nanoparticles: *a*, TEM BF image; *b*, HRTEM image; *c*, EDX analysis; *d*, powder XRD pattern; *e*, HAADF-STEM image.

The surface area of both the catalysts was estimated using the BET method. The surface area of the commercial γ-Al$_2$O$_3$ was found to be 43 m^2/g, whereas that of Pd/Al$_2$O$_3$ and Pt/Al$_2$O$_3$ was 34 and 28 m^2/g respectively. These findings further reiterate that some of the surface regions of the oxide support are occupied by metal nanoparticles.

Silica-supported Pd and Pt nanoparticles

In a manner similar to the synthesis of alumina-supported Pd and Pt nanoparticles, we prepared and characterized Pd and Pt nanoparticles supported on silica. The TEM BF image (Figure 3 *a*) of the Pd/SiO$_2$ sample evidenced the presence of Pd nanoparticles on the silica surface. Unlike the case of Pd/Al$_2$O$_3$, we noted that the Pd nanoparticles are well separated in the case of Pd/SiO$_2$; however, the particles are large. The average particle size was found to be 34.7 ± 0.9 nm. The powder XRD pattern (Figure 3 *b*) of the sample shows a broad hump around 2θ 20–30° due to amorphous silica. The peaks present at 2θ 39.9°, 46.4° and 67.8° could be assigned to the (111), (200) and (220) planes of FCC Pd(0).

The TEM BF image (Figure 4 *a*) of the Pt/SiO$_2$ nanoparticles shows the presence of spherical Pt nanoparticles on the silica support. In contrast to the Pt/Al$_2$O$_3$ sample,
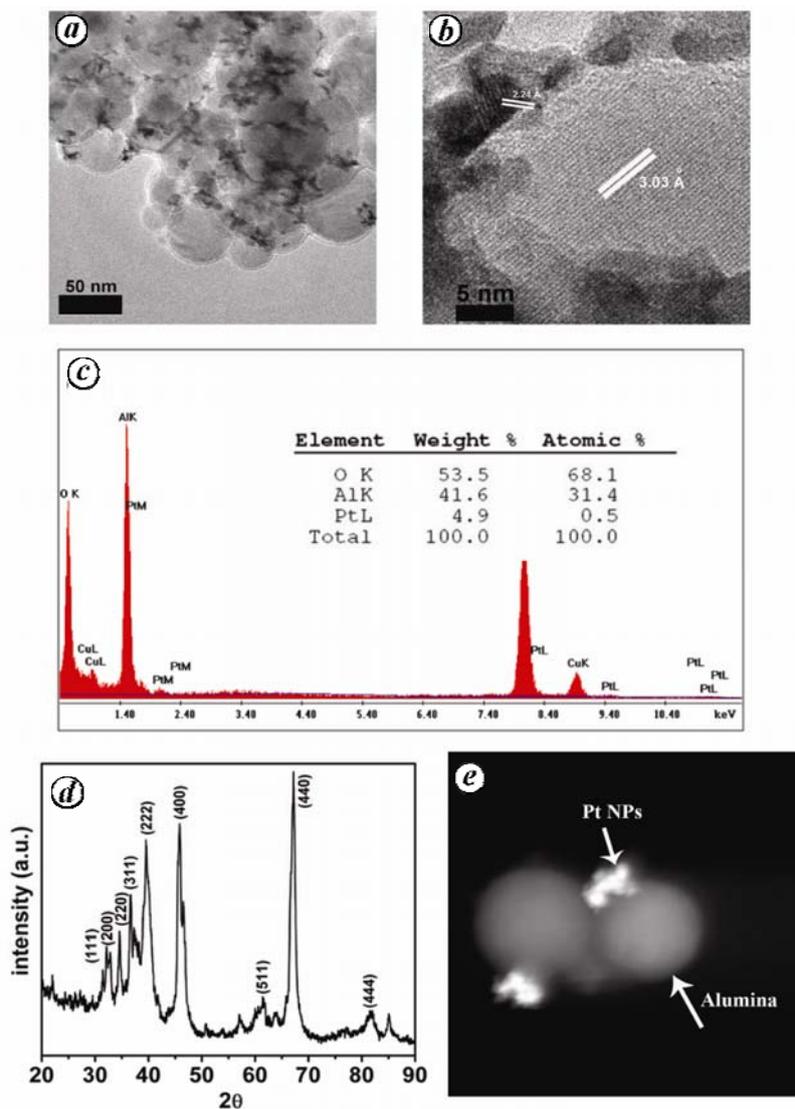
Figure 2. Pt/Al$_2$O$_3$ nanoparticles: *a*, TEM BF image; *b*, HRTEM image; *c*, EDX analysis; *d*, powder XRD pattern; *e*, HAADF-STEM image.

here the Pt nanoparticles are quite monodisperse and well separated in nature. The particle size calculated in this case was 6.3 ± 0.9 nm. Here as well, we did not find any region where the particles were present without the support material. The powder XRD pattern of this sample (Figure 4 *b*) shows a broad hump around 2θ 20–30° due to the amorphous nature of silica. The peaks present at 2θ 39.7°, 46.3° and 67.5° could be assigned to the (111), (200) and (220) planes of FCC Pt(0). The small size of the crystallites was evident from the broad nature of the powder XRD peaks.

The surface area of both the catalysts was estimated from the N$_2$ adsorption–desorption isotherms. The surface area of aerosol 300 silica was found to be 300 m^2/g, whereas it was 183.37 and 250.68 m^2/g for Pd/SiO$_2$ and Pt/SiO$_2$ respectively. Reduction in the surface areas of the catalysts compared to silica could be attributed to the presence of metal nanoparticles in the pores present on

silica. The lower surface area of Pd on silica compared to that of Pt/SiO$_2$ is due to the larger particle size of Pd nanoparticles in comparison to that of Pt nanoparticles (see above).

Discussion

Conventional methods of supported metal nanoparticles reported to date, such as wet impregnation, co-precipitation and precipitation–deposition or colloidal metal nanoparticles grafted on a suitable support suffer from several disadvantages. The lack of control over particle size and size distribution, especially at higher metal loading and removal of the stabilizing agent, generally known to block the active sites of the catalyst, under mild condition are the two primary issues. Thus a sustainable preparative route for the synthesis of supported metal nanostructures that could circumvent these issues is being
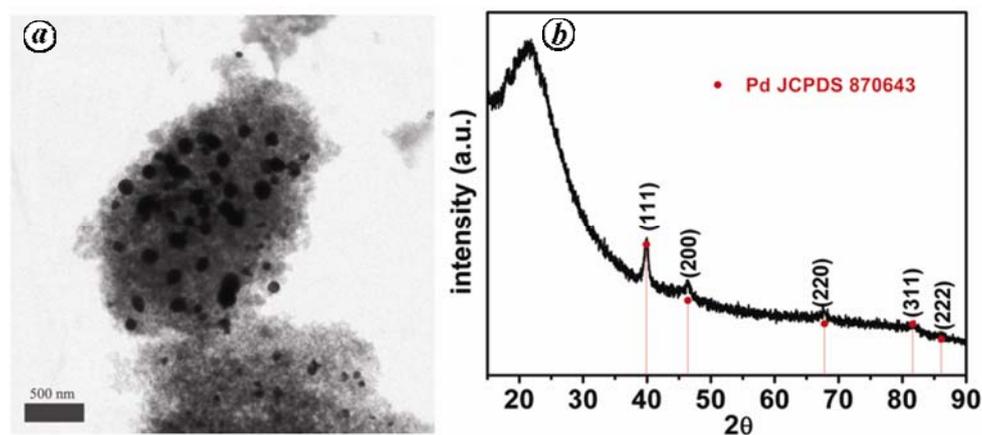
Figure 3. Pd/SiO₂ nanoparticles: *a*, TEM BF image; *b*, Powder XRD pattern.
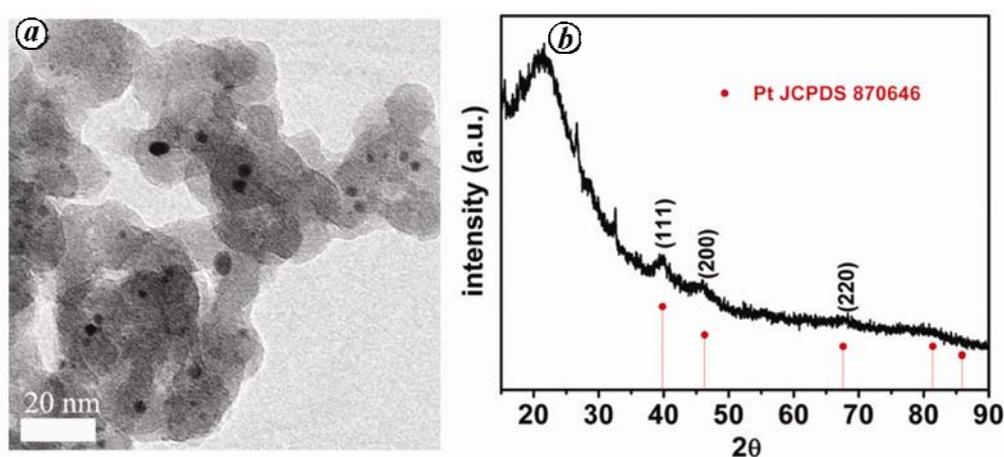

Figure 4. Pt/SiO₂ nanoparticles: *a*, TEM BF image; *b*, Powder XRD pattern.

sought after. A method wherein a capping agent/passivating agent is generated *in situ*, which could further be removed easily by washing with a solvent at room temperature so that sintering of particles could be prevented would be greatly beneficial in this regard. In our continuing efforts towards the development of a sustainable chemical route for the synthesis of metal nanostructures[22], we found that AB is a promising and sustainable reducing agent which affects the reduction of the metal salt in solution as well as in the solid state[19–21]. In the solid-state reduction method it was found that AB acts as a reducing agent and simultaneously generates the stabilizing agent, BNH$_x$ polymer, which essentially halts the growth of the metal nanoparticles that are formed. Recently, Kalidindi *et al.*[21] showed that coinage metal (Cu, Ag and Au) nanoparticles and other noble metal (Pd, Pt and Ir) nanoparticles embedded in BNH$_x$ could be synthesized successfully by this method. In the present work, we adopted a similar methodology. The metal ions were initially grafted on the support materials (γ-alumina and silica) and then they were reduced using AB in the solid

state resulting in the formation of metal nanoparticles encapsulated by the BNH$_x$ polymer and dispersed on the alumina or silica surface. The B–N bond in AB is unstable in aqueous or methanol medium in the presence of a metal nanocatalyst; it undergoes hydrolysis or methanolysis readily to give the borate species. Recently, Demirci *et al.*[30] have shown that BNH$_x$ polymer also could be hydrolysed to afford ammonium borate and hydrogen in the presence of Ru nanoparticles as catalyst. In our case, the powder samples obtained upon reduction of the metal ions using AB on the support materials were washed with methanol repeatedly. In this process, methanolysis of the BNH$_x$ polymer takes place resulting in the formation of ammonium methoxy borate salt, which gets washed out in methanol. Thus the initial stabilizing agent, BNH$_x$ polymer, can be completely removed by washing the powder several times with methanol, finally affording metal nanoparticles dispersed on the support materials. The particle size as well as size distribution can be controlled because of the presence of the stabilizing agent, which makes the process independent of the amount of

metal loading. At the same time, the stabilizing agent could be removed easily by chemical means under mild condition, i.e. at room temperature, thus preventing any sintering of particles. Thus, the synthetic route that we have developed here overcomes some of the problems as outlined above and this protocol is likely to be sustainable for a variety of systems.

Conclusion

In conclusion, we have demonstrated a new synthetic methodology by which γ-alumina and silica-supported Pt and Pd nanoparticles have been synthesized. By this procedure metal ions were adsorbed on the surface of the support materials and then AB was used to reduce the metal ions to realize the metal nanoparticles encapsulated in BNH_x polymer on the support in a totally solid-state reduction method. Here, AB plays a dual role: it acts as a reducing agent and also as a precursor of the BNH_x polymer which controls the growth and size of the nanoparticles formed. The polymer could be removed by repeated methanol washings, resulting in well-dispersed metal nanoparticles on oxide supports. As the size control could be achieved by the BNH_x polymer, it is further possible to improve the catalyst loading without affecting the size distribution of the metal nanoparticles, and hence rendering a sustainable pathway towards the development of new synthetic methodologies for supported metal nanoparticles.

1. Schmid, G., *Nanoparticles: From Theory to Application*, Wiley-VCH, Weinheim, 2004.
2. Klabunde, K. J., *Nanoscale Materials in Chemistry*, Wiley-Interscience, New York, 2001.
3. Hyeon, T., Chemical synthesis of magnetic nanoparticles. *Chem. Commun.*, 2003, 927–934.
4. Dahl, J. A., Maddux, B. L. S. and Hutchinson, J. E., Toward greener nanosynthesis. *Chem. Rev.*, 2007, **107**, 2228–2269.
5. Astruc, D., Lu, F. and Aranzaes, J. R., Nanoparticles as recyclable catalysts: the frontier between homogeneous and heterogeneous catalysis. *Angew. Chem. Int. Ed. Engl.*, 2005, **44**, 7852–7872.
6. Klingelhofer, W., Heitz, A., Greiner, A., Oestreich, S., Foster, S. and Antonietti, M., Preparation of palladium colloids in block copolymer micelles and their use for the catalysis of the Heck reaction. *J. Am. Chem. Soc.*, 1997, **119**, 10116–10120.
7. White, R. J., Luque, R., Budarin, V., Clark, J. H. and Macquarrie, D. J., Supported metal nanoparticles on porous materials. Methods and applications. *Chem. Soc. Rev.*, 2009, **38**, 481–494.
8. Haruta, M., Tsubota, S., Kobayashi, T., Kageyama, H., Genet, M. J. and Delmon, B., Low-temperature oxidation of CO over gold supported on TiO_2, α-Fe_2O_3, and Co_3O_4. *J. Catal.*, 1993, **144**, 175–192.
9. Valden, M., Lai, X. and Goodman, D. W., Onset of catalytic activity of gold clusters on titania with the appearance of nonmetallic properties. *Science*, 1998, **281**, 1647–1650.
10. Heiz, U. and Bullock, E. L., Fundamental aspects of catalysis on supported metal clusters. *J. Mater. Chem.*, 2004, **14**, 564–577.
11. Schwarz, J. A., Contescu, C. and Contescu, A., Methods for preparation of catalytic materials. *Chem. Rev.*, 1995, **95**, 477–510.
12. Toebes, M. L., van Dillen, J. A. and de Jong, Y. P., Synthesis of supported palladium catalysts. *J. Mol. Catal. A*, 2001, **173**, 75–98.
13. Lopez, T., Asomoza, M., Bosch, P., Garciafigueroa, E. and Gomez, R., Spectroscopic characterization and catalytic properties of sol–gel Pd/SiO_2 catalysts. *J. Catal.*, 1992, **138**, 463–473.
14. Xie, Y., Ding, K. L., Liu, Z. M., Tao, R. T., Sun, Z. Y., Zhang, H. Y. and An, G., *In situ* controllable loading of ultrafine noble metal particles on titania. *J. Am. Chem. Soc.*, 2009, **131**, 6648–6649.
15. Okamoto, K., Akiyama, R., Yoshida, H., Yoshida, T. and Kobayashi, S., Formation of nanoarchitectures including subnanometer palladium clusters and their use as highly active catalysts. *J. Am. Chem. Soc.*, 2005, **127**, 2125–2135.
16. Gude, K. and Narayanan, R., Synthesis and characterization of colloidal-supported metal nanoparticles as potential intermediate nanocatalysts. *J. Phys. Chem. C*, 2010, **114**, 6356–6362.
17. Chao, L. C. and Andres, R. P., Synthesis of a supported metal catalyst using nanometer-size clusters. *J. Colloid Interface Sci.*, 1994, **165**, 290–295.
18. Rinaldi, R., Porcari, A. D., Rocha, T. C. R., Cassinelli, W. H., Ribeiro, R. U., Bueno, J. M. C. and Zanchet, D., Construction of heterogeneous Ni catalysts from supports and colloidal nanoparticles – a challenging puzzle. *J. Mol. Catal. A*, 2009, **301**, 11–17.
19. Kalidindi, S. B., Indirani, M. and Jagirdar, B. R., First row transition metal ion-assisted ammonia–borane hydrolysis for hydrogen generation. *Inorg. Chem.*, 2008, **47**, 7424–7429.
20. Kalidindi, S. B., Vernekar, A. A. and Jagirdar, B. R., Co–Co_2B, Ni–Ni_3B and Co–Ni–B nanocomposites catalyzed ammonia–borane methanolysis for hydrogen generation. *Phys. Chem. Chem. Phys.*, 2009, **11**, 770–775.
21. Kalidindi, S. B., Sanyal, U. and Jagirdar, B. R., Metal nanoparticles via atom-economy green approach. *Inorg. Chem.*, 2010, **49**, 3965–3967.
22. Kalidindi, S. B., Sanyal, U. and Jagirdar, B. R., Chemical synthesis of metal nanoparticles using amine–boranes. *ChemSusChem*, 2011, **4**, 317–324.
23. Ramachandran, P. V. and Gagare, P. D., Preparation of ammonia borane in high yield and purity, methanolysis, and regeneration. *Inorg. Chem.*, 2007, **46**, 7810–7817.
24. Haruta, M., Size- and support-dependency in the catalysis of gold. *Catal. Today*, 1997, **36**, 153–166.
25. Bond, G. C. and Thompson, D. T., Catalysis by gold. *Catal. Rev. Sci. Eng.*, 1999, **41**, 319–388.
26. Sanchez, A., Abbet, S., Heiz, U., Schneider, W.-D., HIkkinen, H., Barnett, R. N. and Landman, U., When gold is not noble: nanoscale gold catalysts. *J. Phys. Chem. A*, 1999, **103**, 9573–9578.
27. Barau, A. *et al.*, A simple and efficient route to active and dispersed silica supported palladium nanoparticles. *Catal. Lett.*, 2008, **124**, 204–214.
28. Campelo, J. M., Lee, A. F., Luna, D., Luque, R., Marinas, J. M. and Romero, A. A., Preparation of highly active and dispersed platinum nanoparticles on mesoporous Al-MCM-48 and their activity in the hydroisomerisation of *n*-octane. *Chem. Eur. J.*, 2008, **14**, 5988–5995.
29. Chen, X., Zhu, H. Y., Zhao, J. C., Zheng, Z. F. and Gao, X. P., Visible-light-driven oxidation of organic contaminants in air with gold nanoparticle catalysts on oxide supports. *Angew. Chem., Int. Ed. Engl.*, 2008, **47**, 5353–5356.
30. Demirci, U. B., Bernard, S., Chiriac, R., Toche, F. and Miele, P., Hydrogen release by thermolysis of ammonia borane NH_3BH_3 and then hydrolysis of its by-product $[BNH_x]$. *J. Power Sources*, 2011, **196**, 279–286.